Data in Brief 30 (2020) 105650

Contents lists available at ScienceDirect

Data in Brief

journal homepage: www.elsevier.com/locate/dib

Data Article

Redox data of ferrocenylcarboxylic acids in dichloromethane and acetonitrile

Pieter J. Swarts, Jeanet Conradie*

Department of Chemistry, PO Box 339, University of the Free State, Bloemfontein, 9300, South Africa

ARTICLE INFO

Article history:
Received 15 April 2020
Revised 22 April 2020
Accepted 23 April 2020
Available online 29 April 2020

Keywords:
Ferrocenyl acids
cyclic voltammetry
oxidation
solvent effect
electronic effect

ABSTRACT

Redox data obtained from cyclic voltammetry experiments of the $Fe^{II/III}$ oxidation of six ferrocenyl carboxylic acids is presented in this data in brief article. Data is obtained from the cyclic voltammograms at scan rates of two orders of magnitude (0.05 – 5.00 Vs^{-1}) using (i) acetonitrile as solvent and tetrabutylammonium hexafluorophosphate as supporting electrolyte and (ii) dichloromethane as solvent and tetrabutylammonium tetrakispentafluorophenylborate, as the electrolyte. Data is reported *versus* the $Fe^{II/III}$ redox couple of ferrocene. For more insight in the reported data, see the related research article "Solvent and substituent effect on Electrochemistry of ferrocenylcarboxylic acids", published in Journal of Electroanalytical Chemistry [1].

* Corresponding author.
E-mail address: conradj@ufs.ac.za (J. Conradie).

https://doi.org/10.1016/j.dib.2020.105650

Specifications Table

Subject	Chemistry
Specific subject area	Electrochemistry
Type of data	Table Image Graph Figure
How data were acquired	Princeton Applied Research PARSTAT 2273 potentiostat running Powersuite software (Version 2.58).
Data format	Raw Analysed
Parameters for data collection	Samples were used as synthesized. All the electrochemical experiments were performed in an M Bruan Lab Master SP glove box under a high purity argon atmosphere (H_2O and $O_2 <$ 10 ppm).
Description of data collection	All electrochemical experiments were done in a 2 ml electrochemical cell containing three-electrodes (a glassy carbon working electrode, a Pt auxiliary electrode and a Pt pseudo reference electrode), connected to a Princeton Applied Research PARSTAT 2273 electrochemical analyser. Data obtained were exported to excel for analysis and diagram preparation.
Data source location	University of the Free State Bloemfontein South Africa
Data accessibility	With the article
Related research article	P.J. Swarts, J. Conradie, Solvent and substituent effect on electrochemistry of ferrocenylcarboxylic acids, J. Electroanal. Chem. (2020) 114164. doi:10.1016/j.jelechem.2020.114164.

Value of the Data

- This data provides detailed electrochemical data for six ferrocenyl carboxylic acids in both DCM and ACN for scan rates over two orders of magnitude (0.05 – 5.0 Vs^{-1}).
- This data illustrates the influence of the solvent used in cyclic voltammetry experiments, on the formal redox potential of Fe of the ferrocenyl group for ferrocenylcarboxylic acids.
- This data illustrates the influence of the solvent on the peak current-voltage separations, ΔE_p, of the Fe oxidation peak of ferrocenyl carboxylic acids.
- This data illustrates the electronic influence of electron-withdrawing carbonyl group on the iron's oxidation potential, depending on how close the carbonyl group is to the iron.
- Accurate redox potential data of these ferrocenyl (Fc) carboxylic acids are important, since they are used as ligands in organometallic complexes.

1. Data

This article presents redox data of six ferrocene-containing carboxylic acids, 1 – 6, reported versus the redox couple ferrocene (Fc) at 0, using decamethylferrocene (DmFc) as internal standard [2], see Figure 1 for the series of complexes of this data study. Cyclic voltammograms obtained in dichloromethane (DCM) and acetonitrile (ACN) for compound 1 – 6, with DmFc as internal standard, are shown in Figure 2–Figure 9. The cyclic voltammograms of DmFc and ferrocene in DCM and ACN are shown in Figure 10 and Figure 11. Electrochemical data obtained from the cyclic voltammograms at scan rates 0.05 Vs^{-1} – 5.00 Vs^{-1} are tabulated in Table 1–Table 12 (0.10 Vs^{-1} data from reference [1]). Presented data is related to the research article "Solvent and substituent effect on Electrochemistry of ferrocenylcarboxylic acids", published in Journal of Electroanalytical Chemistry [1]. The electronic influence of the different carboxylic acids

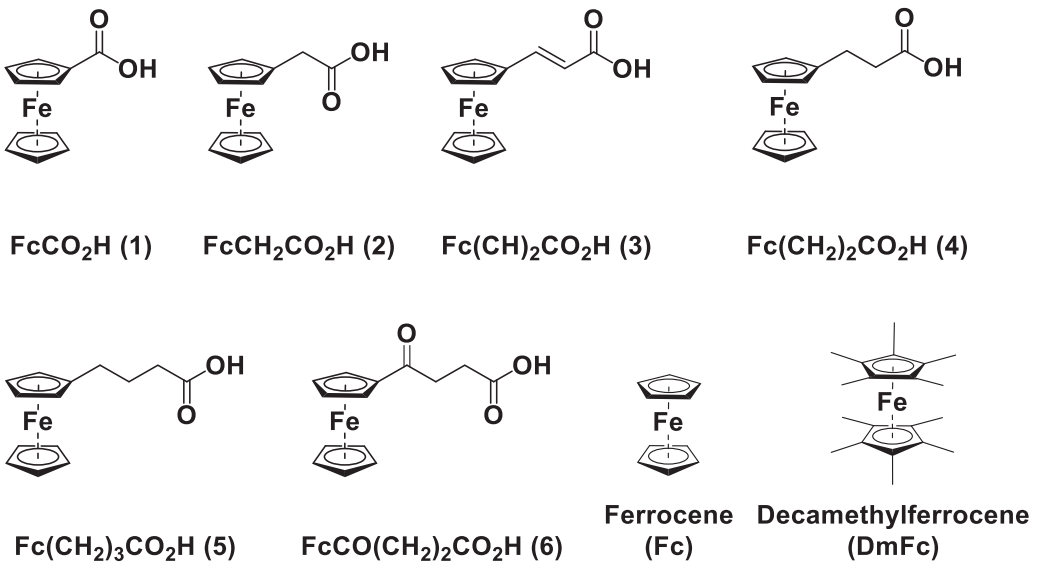

Fig. 1. Structure of compounds in this study used for cyclic voltammetry.

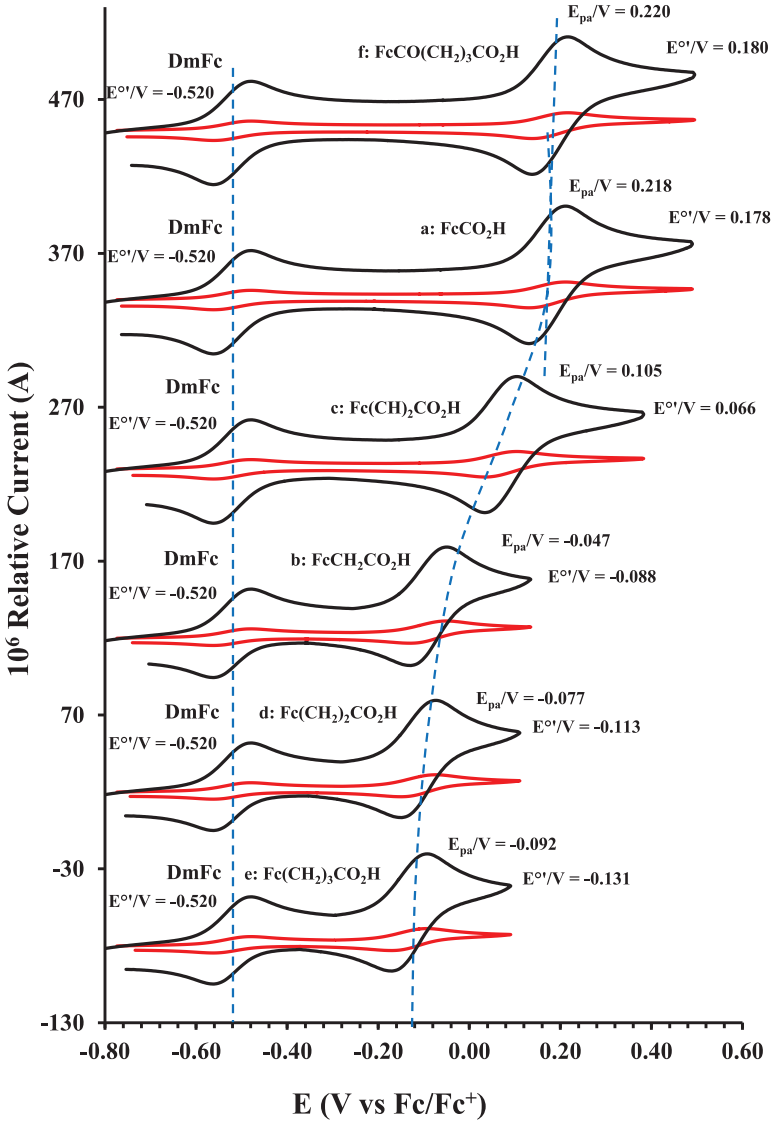

Fig. 2. Cyclic voltammogram in ACN of (a) $FcCO_2H$, (b) $FcCH_2CO_2H$. (c) $Fc(CH)_2CO_2H$, (d) $Fc(CH_2)_2CO_2H$, (e) $Fc(CH_2)_3CO_2H$ and (f) $FcCO(CH_2)_2CO_2H$, at scan rates 0.100 (red) and 5.00 (black) Vs^{-1}. Scans initiated in a positive direction. Data for the peak oxidation potential (E_{pa}) and the formal reduction potential ($E^{0'}$) of DmFc (internal standard, left) and the indicated ferrocene-containing carboxylic acid (right) are indicated in V.

substituents on the redox potential of the ferrocenylgroup they are attached to, is illustrated in Figure 2 and Figure 3. The electronic influence of the electron-withdrawing carbonyl group on the iron's oxidation potential, depends on how close the carbonyl group is to the iron. Redox data of ferrocene-containing compounds are important for application in asymmetric catalysis [3–6], energy transfer processes [7], biological applications [8,9], as additives in highburning rate composite rocket propellants [10] and non-linear optics [6].

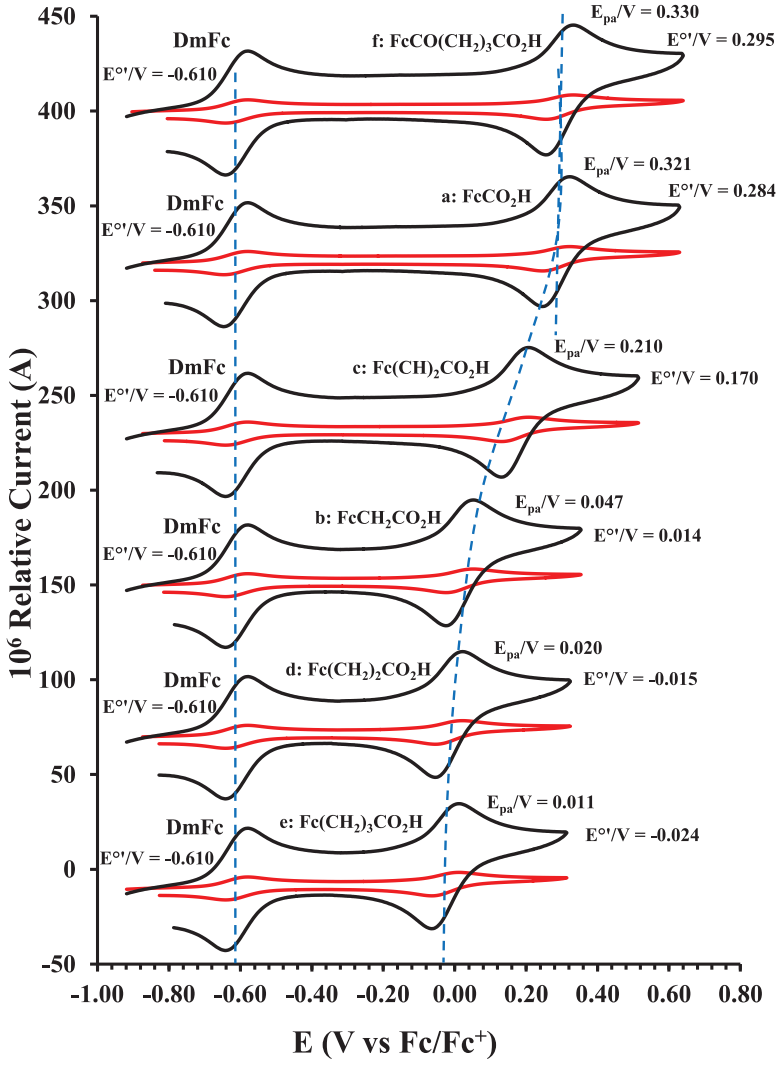

Fig. 3. Cyclic voltammogram in DCM of (a) $FcCO_2H$, (b) $FcCH_2CO_2H$. (c) $Fc(CH)_2CO_2H$, (d) $Fc(CH_2)_2CO_2H$, (e) $Fc(CH_2)_3CO_2H$ and (f) $FcCO(CH_2)_2CO_2H$, at scan rates 0.100 (red) and 5.00 (black) Vs^{-1}. Scans initiated in a positive direction. Data for the peak oxidation potential (E_{pa}) and the formal reduction potential ($E^{0'}$) of DmFc (internal standard, left) and the indicated ferrocene-containing carboxylic acid (right) are indicated in V.

2. Experimental Design, Materials, and Methods

Electrochemical studies through cyclic voltammetry (CV) experiments were performed in an M Bruan Lab Master SP glove box under a high purity argon atmosphere (H_2O and $O_2 < 10$ ppm), utilising a Princeton Applied Research PARSTAT 2273 potentiostat running Powersuite software (Version 2.58). The cyclic voltammetry experimental setup consists of a cell with three electrodes, namely (i) a glassy carbon electrode as working electrode, (ii) a platinum wire auxiliary and (ii) a platinum wire as pseudo reference electrode. The glassy carbon working electrode was polished and prepared before every experiment on a Buhler polishing mat first with 1-micron and then with ¼-micron diamond paste, rinsed with H_2O, acetone and DCM, and dried

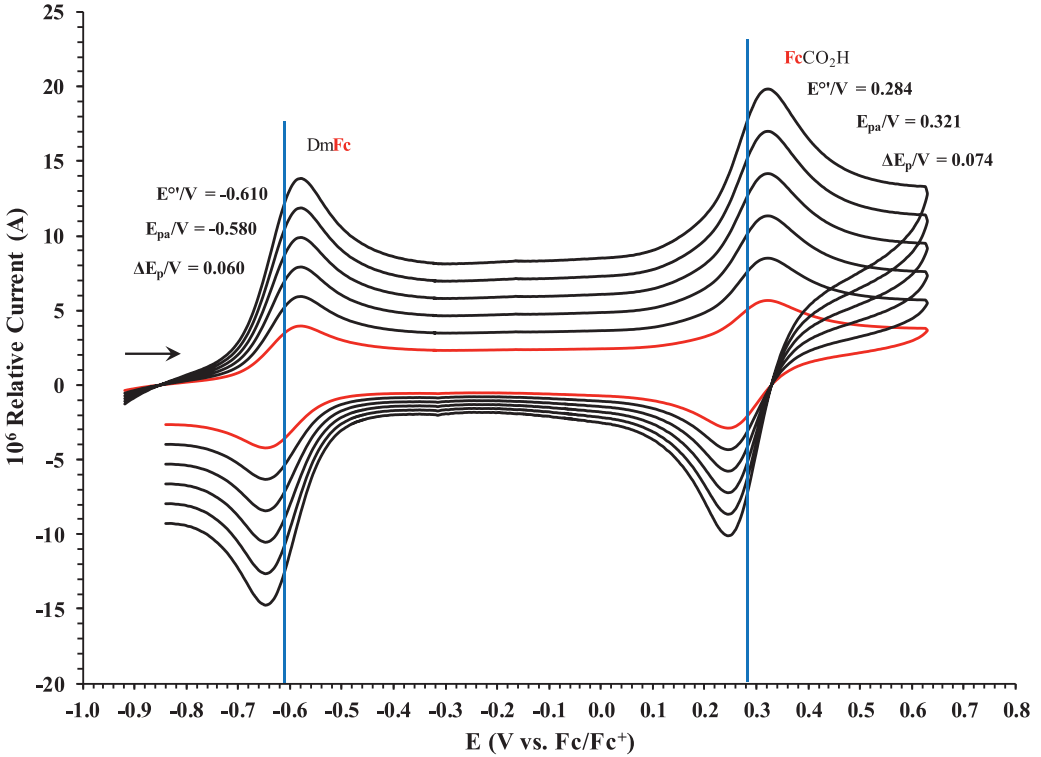

Fig. 4. Cyclic voltammograms in DCM of $FcCO_2H$ at scan rates 0.050 (smallest peak currents), 0.100, 0.200, 0.300, 0.400 and 0.500 (largest peak currents) Vs^{-1}. All scans initiated in a positive direction. Data for the peak oxidation potential (E_{pa}), the formal reduction potential ($E^{0'}$) and the peak current separation ΔE_p of the $Fe^{II/III}$ oxidation of DmFc (internal standard, left) and the indicated ferrocene-containing carboxylic acid (right) are indicated in V.

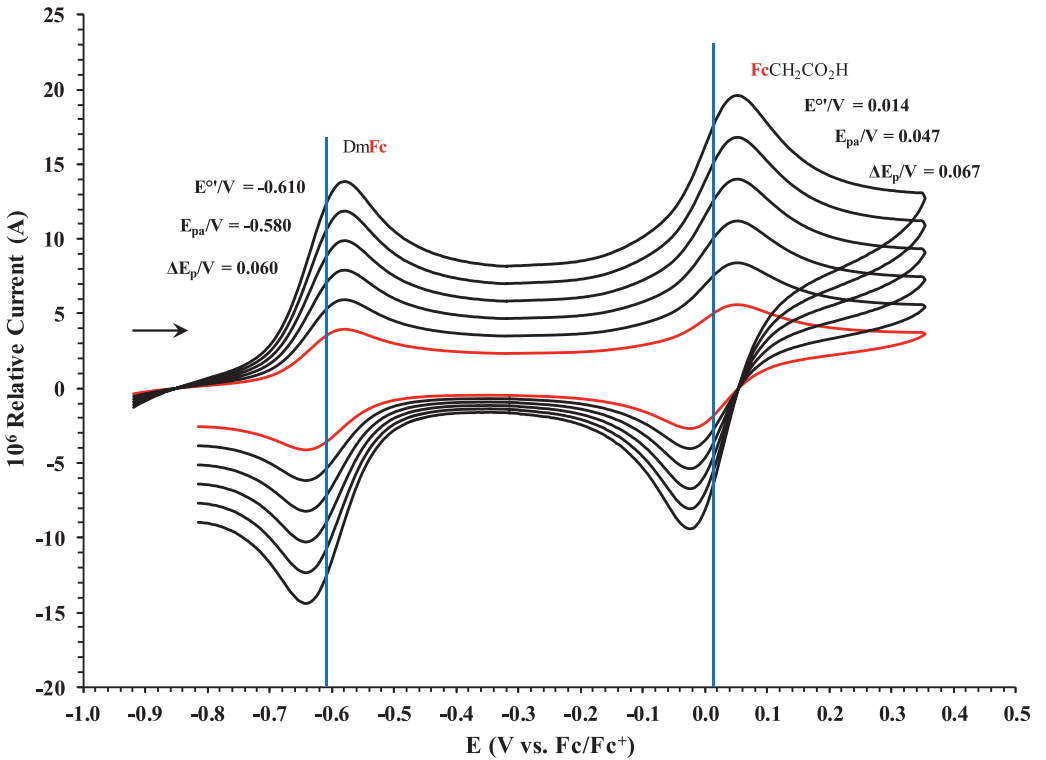

Fig. 5. Cyclic voltammograms in DCM of $FcCH_2CO_2H$ at scan rates 0.050 (smallest peak currents), 0.100, 0.200, 0.300, 0.400 and 0.500 (largest peak currents) Vs^{-1}. All scans initiated in a positive direction. Data for the peak oxidation potential (E_{pa}), the formal reduction potential ($E^{0'}$) and the peak current separation ΔE_p of the $Fe^{II/III}$ oxidation of DmFc (internal standard, left) and the indicated ferrocene-containing carboxylic acid (right) are indicated in V.

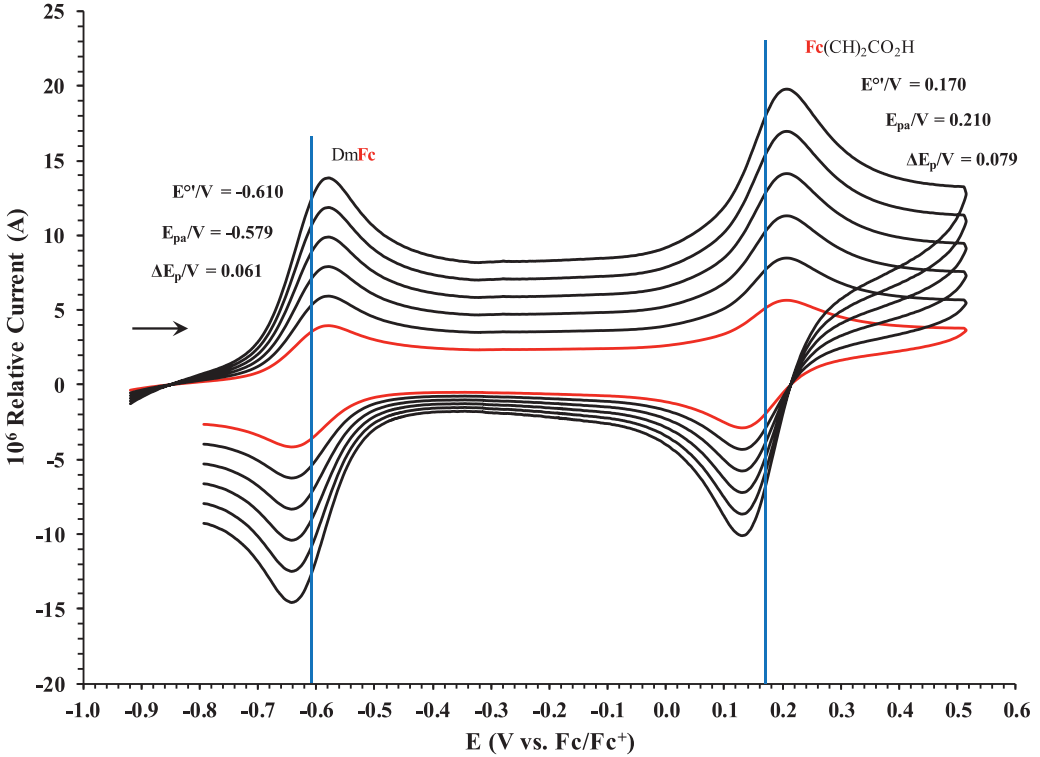

Fig. 6. Cyclic voltammograms in DCM of $Fc(CH)_2CO_2H$ at scan rates 0.050 (smallest peak currents), 0.100, 0.200, 0.300, 0.400 and 0.500 (largest peak currents) Vs^{-1}. All scans initiated in a positive direction. Data for the peak oxidation potential (E_{pa}), the formal reduction potential ($E^{0'}$) and the peak current separation ΔE_p of the $Fe^{II/III}$ oxidation of DmFc (internal standard, left) and the indicated ferrocene-containing carboxylic acid (right) are indicated in V.

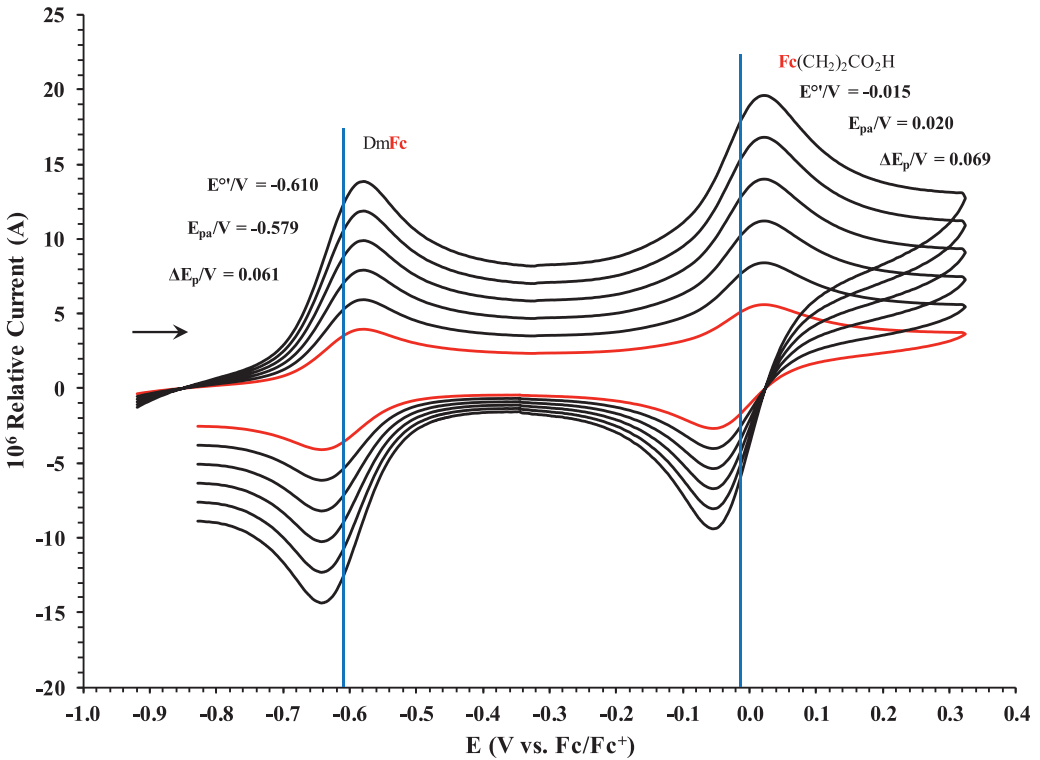

Fig. 7. Cyclic voltammograms in DCM of $Fc(CH_2)_2CO_2H$ at scan rates 0.050 (smallest peak currents), 0.100, 0.200, 0.300, 0.400 and 0.500 (largest peak currents) Vs^{-1}. All scans initiated in a positive direction. Data for the peak oxidation potential (E_{pa}), the formal reduction potential ($E^{0'}$) and the peak current separation ΔE_p of the $Fe^{II/III}$ oxidation of DmFc (internal standard, left) and the indicated ferrocene-containing carboxylic acid (right) are indicated in V.

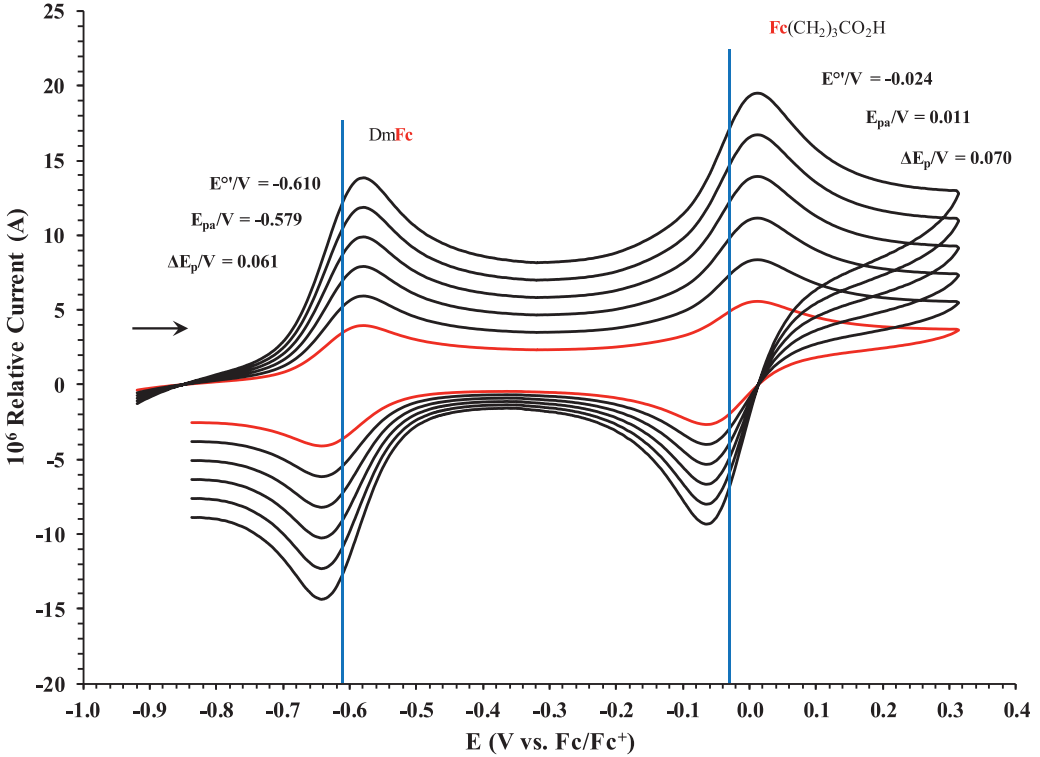

Fig. 8. Cyclic voltammograms in DCM of $Fc(CH_2)_3CO_2H$ at scan rates 0.050 (smallest peak currents), 0.100, 0.200, 0.300, 0.400 and 0.500 (largest peak currents) Vs^{-1}. All scans initiated in a positive direction. Data for the peak oxidation potential (E_{pa}), the formal reduction potential ($E^{0'}$) and the peak current separation ΔE_p of the $Fe^{II/III}$ oxidation of DmFc (internal standard, left) and the indicated ferrocene-containing carboxylic acid (right) are indicated in V.

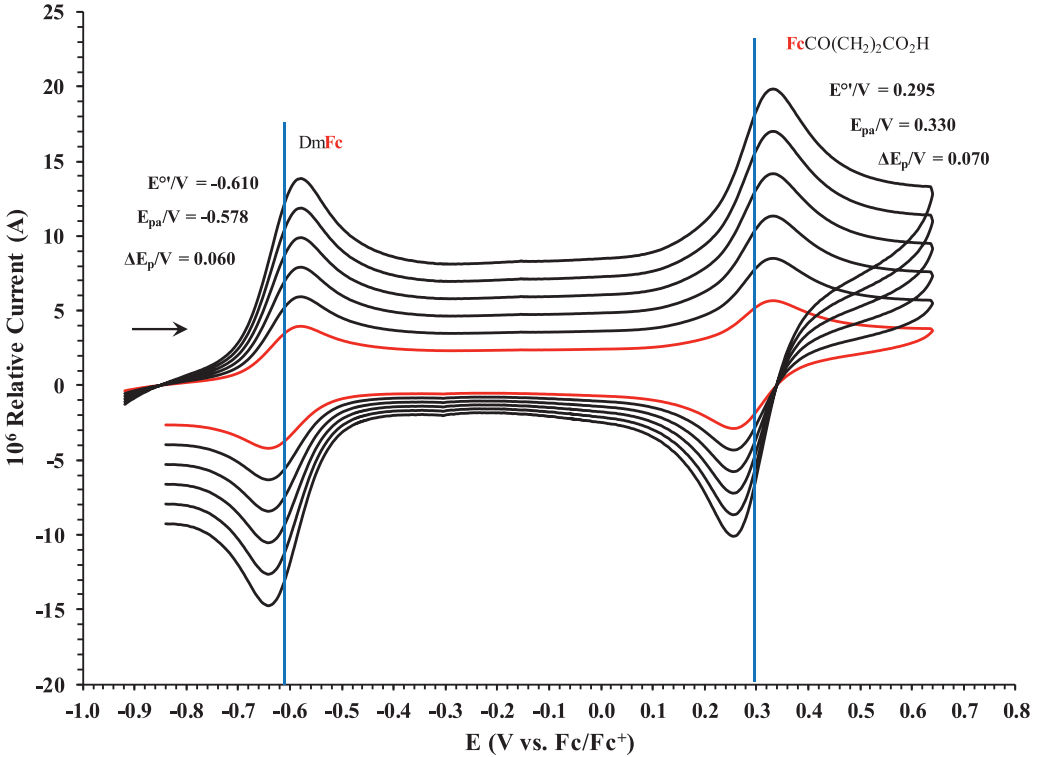

Fig. 9. Cyclic voltammograms in DCM of $FcCO(CH_2)_2CO_2H$at scan rates 0.050 (smallest peak currents), 0.100, 0.200, 0.300, 0.400 and 0.500 (largest peak currents) Vs^{-1}. All scans initiated in a positive direction. Data for the peak oxidation potential (E_{pa}), the formal reduction potential ($E^{0'}$) and the peak current separation ΔE_p of the $Fe^{II/III}$ oxidation of DmFc (internal standard, left) and the indicated ferrocene-containing carboxylic acid (right) are indicated in V.

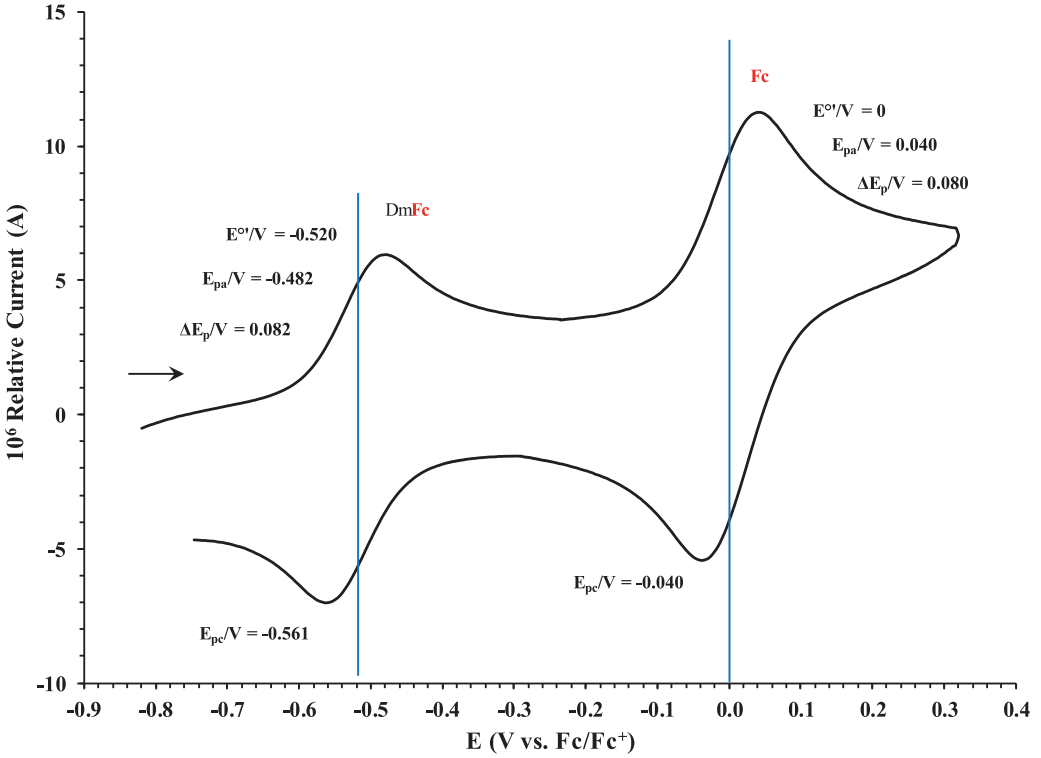

Fig. 10. Cyclic voltammograms in ACN of decamethylferrocene and ferrocene at scan rate 0.100 Vs^{-1}. The scan is initiated in a positive direction. Data for the peak oxidation potential (E_{pa}), the formal reduction potential ($E^{0'}$) and the peak current separation ΔE_p of the $Fe^{II/III}$ oxidation of DmFc (internal standard, left) and Fc (right) is indicated in V.

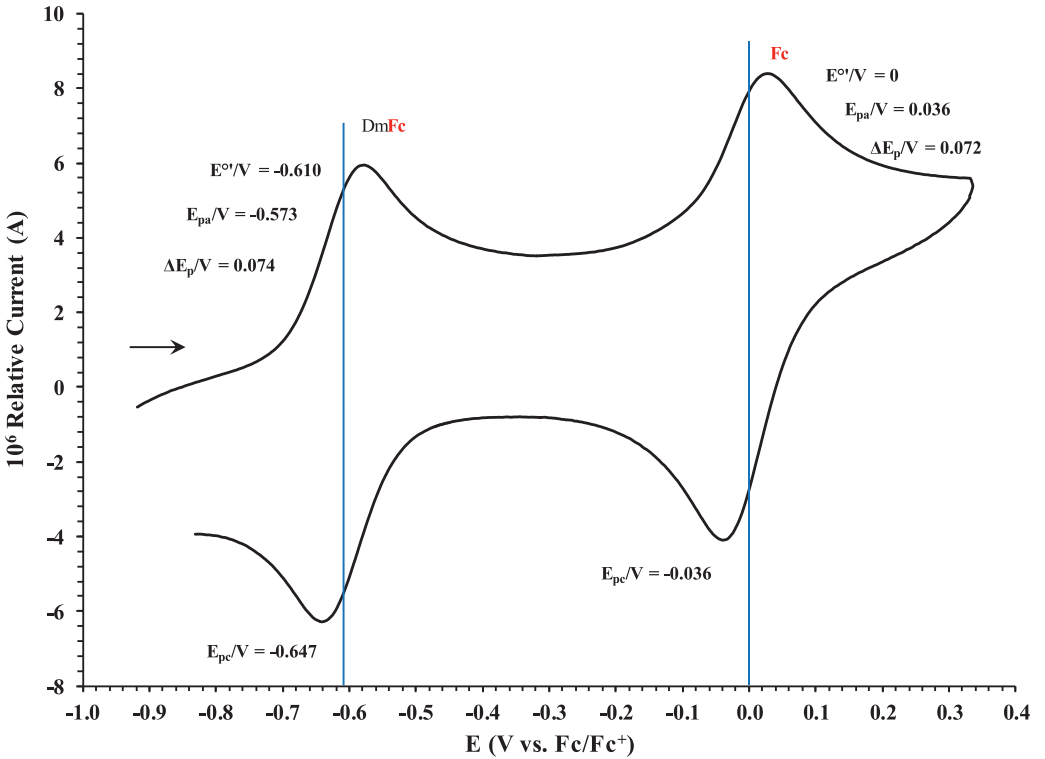

Fig. 11. Cyclic voltammograms in DCM of decamethylferrocene and ferrocene at scan rate 0.100 Vs^{-1}. The scan is initiated in a positive direction. Data for the peak oxidation potential (E_{pa}), the formal reduction potential ($E^{0'}$) and the peak current separation ΔE_p of the $Fe^{II/III}$ oxidation of DmFc (internal standard, left) and Fc (right) is indicated in V.

Table 1
Electrochemical data (potential in V *vs* Fc/Fc^+) in ACN for *c.a.* 5×10^{-4} mol dm^{-3} of $FcCO_2H$ at indicated scan rates (ν in V/s).

ν (V/s)	E_{pa} / V	ΔE_p / V	$E^{o'}$ / V	i_{pa} / μA	i_{pc}/i_{pa}
DmFc					
0.100	**-0.480**	**0.080**	**-0.520**	**3.21**	**0.99**
$FcCO_2H$					
0.050	0.217	0.078	0.178	2.16	0.99
0.100	**0.218**	**0.080**	**0.178**	**3.86**	**0.99**
0.200	0.218	0.080	0.178	5.54	0.99
0.300	0.218	0.080	0.178	6.59	0.99
0.400	0.219	0.082	0.178	8.01	0.99
0.500	0.219	0.082	0.178	9.04	0.99
5.000	0.220	0.084	0.178	26.91	0.99

Table 2
Electrochemical data (potential in V *vs* Fc/Fc^+) in DCM for *c.a.* 5×10^{-4} mol dm^{-3} of $FcCO_2H$ at indicated scan rates (ν in V/s).

ν (V/s)	E_{pa} / V	ΔE_p / V	$E^{o'}$ / V	i_{pa} / μA	i_{pc}/i_{pa}
DmFc					
0.100	**-0.580**	**0.060**	**-0.610**	**3.47**	**0.99**
$FcCO_2H$					
0.050	0.320	0.072	0.284	2.33	0.99
0.100	**0.321**	**0.074**	**0.284**	**3.60**	**0.99**
0.200	0.321	0.074	0.284	5.62	0.99
0.300	0.321	0.074	0.284	6.80	0.99
0.400	0.322	0.076	0.284	8.16	0.99
0.500	0.322	0.076	0.284	9.14	0.99
5.000	0.323	0.078	0.284	25.27	0.99

Table 3
Electrochemical data (potential in V *vs* Fc/Fc^+) in ACN for *c.a.* 5×10^{-4} mol dm^{-3} of $FcCH_2CO_2H$ at indicated scan rates (ν in V/s).

ν (V/s)	E_{pa} / V	ΔE_p / V	$E^{o'}$ / V	i_{pa} / μA	i_{pc}/i_{pa}
DmFc					
0.100	**-0.481**	**0.078**	**-0.520**	**3.35**	**0.99**
$FcCH_2CO_2H$					
0.050	-0.048	0.080	-0.088	2.31	0.99
0.100	**-0.047**	**0.082**	**-0.088**	**3.57**	**0.99**
0.200	-0.047	0.083	-0.088	4.29	0.99
0.300	-0.046	0.084	-0.088	6.45	0.99
0.400	-0.046	0.085	-0.088	8.15	0.99
0.500	-0.045	0.086	-0.088	10.22	0.99
5.000	-0.043	0.090	-0.088	27.12	0.99

before each experiment. The electrochemical analysis is performed in dichloromethane (DCM, anhydrous, $\geq$ 99.8%, containing 40-150 ppm amylene as a stabilizer) and in acetonitrile (ACN, anhydrous, 99.8%) as solvents, at RT. Solutions were made in 0.001 dm^3 spectrochemical grade anhydrous DCM or ACN containing ca. 5×10^{-4} M of analyte, 5×10^{-4} mol dm^{-3} of internal reference (decamethylferrocene, DmFc) and 0.1 mol dm^{-3} of supporting electrolyte tetrabutylammonium tetrakispentafluorophenylborate, $[N(^nBu)_4][B(C_6F_5)_4]$ in DCM, or tetrabutylammonium hexafluorophosphate, $TBAPF_6$, $[N(^nBu)_4][PF_6]$ in ACN. Experimental potential data was measured *vs.* the redox couple of decamethylferrocene DmFc as internal standard [2] and reported vs. the redox couple of ferrocene, Fc, as suggested by IUPAC [11]. $E^{o'}(DmFc) = -0.610$ V vs. Fc/Fc^+ at 0 V in $DCM/[N(Bu)_4][B(C_6F_5)_4]$ and -0.520 vs. Fc/Fc^+ at 0 V in $ACN/[N(Bu)_4][PF_6]$. Scan rates were between 0.05 and 5.00 Vs^{-1}.

Table 4
Electrochemical data (potential in V *vs* Fc/Fc^+) in DCM for *c.a.* 5×10^{-4} mol dm^{-3} of $FcCH_2CO_2H$ at indicated scan rates (ν in V/s).

ν (V/s)	E_{pa} / V	ΔE_p / V	$E^{o'}$ / V	i_{pa} / μA	i_{pc}/i_{pa}
DmFc					
0.100	**-0.580**	**0.060**	**-0.610**	**3.65**	**0.99**
$FcCH_2CO_2H$					
0.050	0.046	0.065	0.014	2.21	0.99
0.100	**0.047**	**0.067**	**0.014**	**3.78**	**0.99**
0.200	0.047	0.068	0.014	4.35	0.99
0.300	0.047	0.068	0.014	6.25	0.99
0.400	0.047	0.069	0.014	8.24	0.99
0.500	0.048	0.070	0.014	10.51	0.99
5.000	0.049	0.072	0.014	25.72	0.99

Table 5
Electrochemical data (potential in V *vs* Fc/Fc^+) in ACN for *c.a.* 5×10^{-4} mol dm^{-3} of $Fc(CH)_2CO_2H$ at indicated scan rates (ν in V/s).

ν (V/s)	E_{pa} / V	ΔE_p / V	$E^{o'}$ / V	i_{pa} / μA	i_{pc}/i_{pa}
DmFc					
0.100	**-0.480**	**0.080**	**-0.520**	**3.82**	**0.99**
$Fc(CH)_2CO_2H$					
0.050	0.104	0.076	0.066	2.01	0.99
0.100	**0.105**	**0.078**	**0.066**	**3.93**	**0.99**
0.200	0.105	0.078	0.066	4.84	0.99
0.300	0.105	0.078	0.066	6.48	0.99
0.400	0.106	0.080	0.066	7.85	0.99
0.500	0.106	0.080	0.066	8.84	0.99
5.000	0.107	0.082	0.066	26.87	0.99

Table 6
Electrochemical data (potential in V *vs* Fc/Fc^+) in DCM for *c.a.* 5×10^{-4} mol dm^{-3} of $Fc(CH)_2CO_2H$ at indicated scan rates (ν in V/s).

ν (V/s)	E_{pa} / V	ΔE_p / V	$E^{o'}$ / V	i_{pa} / μA	i_{pc}/i_{pa}
DmFc					
0.100	**-0.579**	**0.061**	**-0.610**	**3.25**	**0.99**
$Fc(CH)_2CO_2H$					
0.050	0.209	0.078	0.170	1.98	0.99
0.100	**0.210**	**0.079**	**0.170**	**3.36**	**0.99**
0.200	0.210	0.079	0.170	4.91	0.99
0.300	0.210	0.079	0.170	6.54	0.99
0.400	0.211	0.080	0.170	7.94	0.99
0.500	0.211	0.080	0.170	8.94	0.99
5.000	0.212	0.084	0.170	25.58	0.99

Table 7
Electrochemical data (potential in V *vs* Fc/Fc^+) in ACN for *c.a.* 5×10^{-4} mol dm^{-3} of $Fc(CH_2)_2CO_2H$ at indicated scan rates (ν in V/s).

ν (V/s)	E_{pa} / V	ΔE_p / V	$E^{o'}$ / V	i_{pa} / μA	i_{pc}/i_{pa}
DmFc					
0.100	**-0.482**	**0.076**	**-0.520**	**3.58**	**0.99**
$Fc(CH_2)_2CO_2H$					
0.050	-0.078	0.070	-0.113	2.22	0.99
0.100	**-0.077**	**0.072**	**-0.113**	**3.74**	**0.99**
0.200	-0.077	0.073	-0.113	4.84	0.99
0.300	-0.076	0.074	-0.113	6.48	0.99
0.400	-0.076	0.075	-0.113	8.39	0.99
0.500	-0.075	0.076	-0.113	9.55	0.99
5.000	-0.074	0.078	-0.113	26.71	0.99

Table 8
Electrochemical data (potential in V *vs* Fc/Fc^+) in DCM for *c.a.* 5×10^{-4} mol dm^{-3} of $Fc(CH_2)_2CO_2H$ at indicated scan rates (ν in V/s).

ν (V/s)	E_{pa} / V	ΔE_p / V	$E^{o'}$ / V	i_{pa} / μA	i_{pc}/i_{pa}
DmFc					
0.100	**-0.579**	**0.060**	**-0.610**	**3.74**	**0.99**
$Fc(CH_2)_2CO_2H$					
0.050	0.019	0.068	-0.015	2.12	0.99
0.100	**0.020**	**0.070**	**-0.015**	**3.87**	**0.99**
0.200	0.020	0.070	-0.015	5.11	0.99
0.300	0.020	0.070	-0.015	6.73	0.99
0.400	0.021	0.072	-0.015	8.01	0.99
0.500	0.021	0.072	-0.015	9.11	0.99
5.000	0.022	0.074	-0.015	25.32	0.99

Table 9
Electrochemical data (potential in V *vs* Fc/Fc^+) in ACN for *c.a.* 5×10^{-4} mol dm^{-3} of $Fc(CH_2)_3CO_2H$ at indicated scan rates (ν in V/s).

ν (V/s)	E_{pa} / V	ΔE_p / V	$E^{o'}$ / V	i_{pa} / μA	i_{pc}/i_{pa}
DmFc					
0.100	**-0.482**	**0.075**	**-0.520**	**3.64**	**0.99**
$Fc(CH_2)_3CO_2H$					
0.050	-0.091	0.077	-0.131	2.52	0.99
0.100	**-0.092**	**0.078**	**-0.131**	**3.83**	**0.99**
0.200	-0.092	0.079	-0.131	5.15	0.99
0.300	-0.092	0.080	-0.131	6.95	0.99
0.400	-0.093	0.081	-0.131	8.35	0.99
0.500	-0.093	0.082	-0.131	9.69	0.99
5.000	-0.094	0.084	-0.131	27.31	0.99

Table 10
Electrochemical data (potential in V *vs* Fc/Fc^+) in DCM for *c.a.* 5×10^{-4} mol dm^{-3} of $Fc(CH_2)_3CO_2H$ at indicated scan rates (ν in V/s).

ν (V/s)	E_{pa} / V	ΔE_p / V	$E^{o'}$ / V	i_{pa} / μA	i_{pc}/i_{pa}
DmFc					
0.100	**-0.579**	**-0.061**	**-0.610**	**3.89**	**0.99**
$Fc(CH_2)_3CO_2H$					
0.050	0.010	0.068	-0.024	2.39	0.99
0.100	**0.011**	**0.070**	**-0.024**	**3.98**	**0.99**
0.200	0.011	0.070	-0.024	5.26	0.99
0.300	0.012	0.072	-0.024	6.82	0.99
0.400	0.012	0.072	-0.024	8.23	0.99
0.500	0.013	0.074	-0.024	9.46	0.99
5.000	0.014	0.076	-0.024	25.04	0.99

Table 11
Electrochemical data (potential in V *vs* Fc/Fc^+) in ACN for *c.a.* 5×10^{-4} mol dm^{-3} of $FcCO(CH_2)_2CO_2H$ at indicated scan rates (ν in V/s).

ν (V/s)	E_{pa} / V	ΔE_p / V	$E^{o'}$ / V	i_{pa} / μA	i_{pc}/i_{pa}
DmFc					
0.100	**-0.480**	**0.080**	**-0.520**	**3.13**	**0.99**
$FcCO(CH_2)_2CO_2H$					
0.050	0.219	0.078	0.180	2.31	0.99
0.100	**0.220**	**0.080**	**0.180**	**3.52**	**0.99**
0.200	0.220	0.080	0.180	5.29	0.99
0.300	0.220	0.080	0.180	6.85	0.99
0.400	0.221	0.082	0.180	8.66	0.99
0.500	0.221	0.082	0.180	9.85	0.99
5.000	0.222	0.084	0.180	27.26	0.99

Table 12
Electrochemical data (potential in V *vs* Fc/Fc^+) in DCM for *c.a.* 5×10^{-4} mol dm^{-3} of $FcCO(CH_2)_2CO_2H$ at indicated scan rates (ν in V/s).

ν (V/s)	E_{pa} / V	ΔE_p / V	$E^{o'}$ / V	i_{pa} / μA	i_{pc}/i_{pa}
DmFc					
0.100	**-0.580**	**0.060**	**-0.610**	**3.51**	**0.99**
$FcCO(CH_2)_2CO_2H$					
0.050	0.329	0.068	0.295	2.42	0.99
0.100	**0.330**	**0.070**	**0.295**	**3.67**	**0.99**
0.200	0.330	0.070	0.295	5.22	0.99
0.300	0.331	0.072	0.295	6.99	0.99
0.400	0.331	0.072	0.295	8.31	0.99
0.500	0.332	0.074	0.295	9.55	0.99
5.000	0.335	0.080	0.295	25.84	0.99

Declaration of Competing Interest

The authors declare that they have no known competing financial interests or personal relationships which have, or could be perceived to have, influenced the work reported in this article.

Acknowledgements

This work has received support from the South African National Research Foundation (Grant numbers 113327 and 96111) and the Central Research Fund of the University of the Free State, Bloemfontein, South Africa.

Supplementary materials

Supplementary material associated with this article can be found, in the online version, at doi:10.1016/j.dib.2020.105650.

References

[1] P.J. Swarts, J. Conradie, Solvent and substituent effect on electrochemistry of ferrocenylcarboxylic acids, J. Electroanal. Chem. (2020) 114164, doi:10.1016/j.jelechem.2020.114164.
[2] I. Noviandri, K.N. Brown, D.S. Fleming, P.T. Gulyas, P.A. Lay, A.F. Masters, L. Phillips, The Decamethylferrocenium/Decamethylferrocene Redox Couple: A Superior Redox Standard to the Ferrocenium/Ferrocene Redox Couple for Studying Solvent Effects on the Thermodynamics of Electron Transfer, J. Phys. Chem. B. 103 (1999) 6713–6722.
[3] J. Conradie, Density functional theory calculations of Rh-β-diketonato complexes, Dalt. Trans. 44 (2015) 1503–1515, doi:10.1039/C4DT02268H.
[4] J. Conradie, G.J. Lamprecht, A. Roodt, J.C. Swarts, Kinetic study of the oxidative addition reaction between methyl iodide and $[Rh(FcCOCHCOCF_3)(CO)(PPh_3)]$: Structure of $[Rh(FcCOCHCOCF_3)(CO)(PPh_3)(CH_3)(I)]$, Polyhedron 26 (2007) 5075–5087, doi:10.1016/j.poly.2007.07.004.
[5] Q. Shen, S. Shekhar, J.P. Stambuli, J.F. Hartwig, Highly reactive, general, and long-lived catalysts for coupling heteroaryl and aryl chlorides with primary nitrogen nucleophiles, Angew. Chemie - Int. Ed. 44 (2005) 1371–1375, doi:10.1002/anie.200462629.
[6] P.T.N. Nonjola, U. Siegert, J.C. Swarts, Synthesis, Electrochemistry and Cytotoxicity of Ferrocene-Containing Amides, Amines and Amino-Hydrochlorides, J. Inorg. Organomet. Polym. Mater. 25 (2015) 376–385, doi:10.1007/s10904-015-0195-4.
[7] F. Spänig, C. Kovacs, F. Hauke, K. Ohkubo, S. Fukuzumi, D.M. Guldi, A. Hirsch, Tuning charge transfer energetics in reaction center mimics via T h-functionalization of fullerenes, J. Am. Chem. Soc. 131 (2009) 8180–8195, doi:10.1021/ja900675t.
[8] J. Conradie, J.C. Swarts, Relationship between electrochemical potentials and substitution reaction rates of ferrocene-containing β-diketonato rhodium (I) complexes; Cytotoxicity of [Rh(FcCOCHCOPh)(cod)], Dalt. Trans. (2011) 40, doi:10.1039/c1dt00013f.

[9] S.C. by Perry Reeves, C.J. by J Mrowca, M.M. Borecki, W.A. Sheppard, Carboxylation of Aromatic Compounds: Ferrocenecarboxylic acid, Org. Synth. Coll. (1988) 6, doi:10.15227/orgsyn.056.0028.
[10] P.J. Swarts, M. Immelman, G.J. Lamprecht, S.E. Greyling, J.C. Swarts, Ferrocene derivatives as high burning rate catalysts in composite propellants, South African, J. Chem. 50 (1997) 208–216.
[11] G. Gritzner, J. Kuta, Recommendations on reporting electrode potentials in nonaqueous solvents (Recommendations 1983), Pure Appl. Chem. 56 (1984) 461–466, doi:10.1351/pac198456040461.